



Enabling Science through European Electron Microscopy

Deliverable 6.2 : "Report on protocols in-situ EDX and EELS"

Expected Delivery date: M30 June 2021
Actual Delivery date: 23rd of June 2021
Lead beneficiary: ZAR
Person responsible: Raul Arenal
Deliverable type: R DEM DEC OTHER ETHICS ORDP
Dissemination level: PU CO EU-RES EU-CON EU-SEC



Grant Agreement No:	823802
Funding Instrument:	Research and Innovation Actions (RIA)
Funded under:	H2020-INFRAIA-2018-1: Integrating Activities for Advanced Communities
Starting date:	01.01.2019
Duration:	48 months

Table of contents

6.2.1: In-situ EELS analysis of graphene oxide samples - Zaragoza *p. 3-10*

6.2.2: In-situ EELS investigations of metal/insulating transitions - Orsay *p. 11*

Revision history log

Version number	Date of release	Authors	Summary of changes
V0.1		Raul Arenal, Mario Pelaez, Simon Hettler	Redaction 6.2.1
V0.2		Laura Bocher	Redaction 6.2.2
V0.2R		Laura Bocher & Raul Arenal	Verifications and corrections
V1	21/06/2021	Peter van Aken	Approval of deliverable

D6.2.1 In-situ EELS analysis of graphene oxide samples - Zaragoza University:

The reduction of GO is a pillar in current nanomaterial research due to the myriad of potential applications it allows. For this, detailed *in-situ* characterisation of GO thin samples as they undergo different procedures (such as, but not limited to, thermal reduction and electrical current) is of extreme importance. In order to maximise the amount of information gained by *in-situ* EELS characterisation, **ZAR** has set in place a complete protocol to estimate the oxidation degree, thickness, mass density and sp^2 fraction in the C atoms of the sample, taking the core-loss and low-loss spectra of the sample as the starting points.

Core-loss: initial calibration

Initially, the core loss spectra have been subjected to a standard calibration, taking the C-K and the O-K edges of the spectra as reference for this calibration. The N-K edge, attributed to dopants in the sample, has been used in place of the O-K edge for heavily reduced samples.

With the purpose of removing the effects of multiple scattering, every background-subtracted core-loss spectrum has undergone a Fourier log-ratio deconvolution¹ with a low-loss spectrum of the identical region of the sample, which can be seen as a point spread function. An example of the effects of this procedure can be seen in Figure 1.

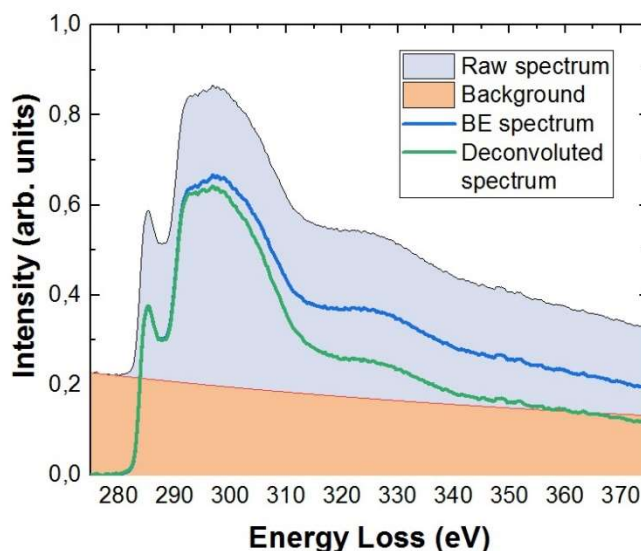


Figure 1: Background subtraction and Fourier log-ratio deconvolution on a core-loss EELS C-K edge.

The analysis of the ELNES features in the C-K and O-K edge of the core-loss spectra corresponding to the oxygen functional groups (OFGs) present in the sample is key for the characterisation of GO samples. Based on previous XPS and EELS studies, as well as studies that focused on the temperature desorption of certain OFGs, we have been able to locate individual features for each OFG²⁻⁶.

In the C-K edge, six different ELNES features can be present, all of them corresponding to π^* transitions. Going up in energy, the features locate at 248.9 eV, 286 eV, 286.6 eV, 287.5 eV, 288.4 eV and 289.4 eV, corresponding, respectively, to sp^2 C, C-OH bonds of hydroxyl groups, C-O bonds in ether and epoxide groups, C-N bonds, C=O bonds in carbonyl groups, and finally to the O-C-OH bonds of carboxyl groups. Depending on the investigated sample, not all of these features are present or resolved due to small differences in energy or might slightly shift in energy. Fig. 2 shows C-K spectra were four OFGs are marked. This Fig. 2 illustrates well the effects of the *in-situ* reduction and how the removal of the OFG can be then monitored.

As for the O-K edge, five ELNES features are found at 531.8 eV, 533.6 eV, 534.9 eV, 536.2 eV and 538.5 eV, corresponding, respectively, to water vibrations, O=C bonds in carbonyl groups, C-O-C bonds of epoxy groups, C-O-C bonds in ether groups and O-H bonds in hydroxyl groups. These features can vary slightly with the sample and their presence will depend on the sample itself. A second feature for water has been found at 534.5 eV⁶. A representation of two spectra, one for GO and another one for rGO, can be seen in Figure 2.

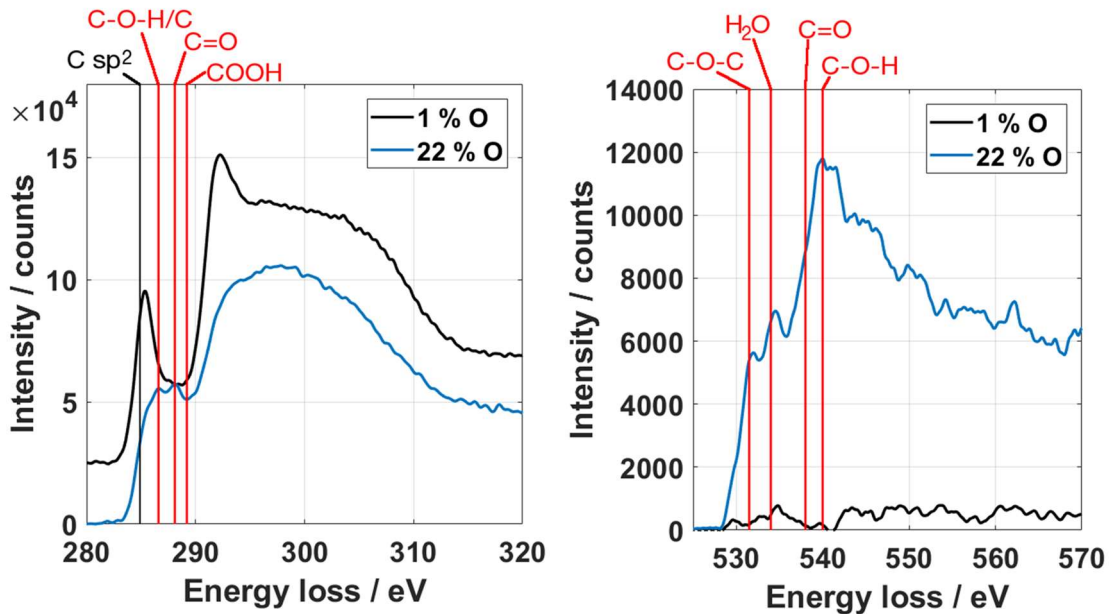


Figure 2: C-K (left) and O-K (right) edges of a heavily oxidised GO sample (blue) and a reduced, via Joule effect, GO sample (black). OFG ELNES features are noted in each spectrum.

Chemical quantification and oxidation degree

The common integration quantification methods for core-loss EELS are used in these studies in order to analyse the relative composition of carbon and oxygen, as well as possible natural dopants (nitrogen) and potential pollutants. These measurements allow for a simple expression of the oxidation rate of the sample, taken as the normalised oxygen ratio with respect to the sum of the carbon and oxygen relative compositions:

$$\%O = \frac{[O]}{[C] + [O]}$$

Thickness estimation

The thickness of the GO samples has been estimated by means of a log-ratio technique¹, applying the following expression, which can be derived from basic optics

$$\frac{t}{\lambda} = \ln\left(\frac{I_t}{I_0}\right)$$

where t is the estimated thickness, λ is the inelastic mean free path (IMFP) of the sample being studied, I_t the transmitted unscattered intensity, and I_0 the incoming intensity.

For the purpose of this analysis, I_0 has been taken as the zero-loss peak of the spectrum and measured by integrating the spectral intensity from -2 to 2 eV. I_t has been taken as the total intensity of the spectrum and measured by integrating the spectral intensity from -2 to 100 eV. A visual representation of these windows can be seen in Figure 3.

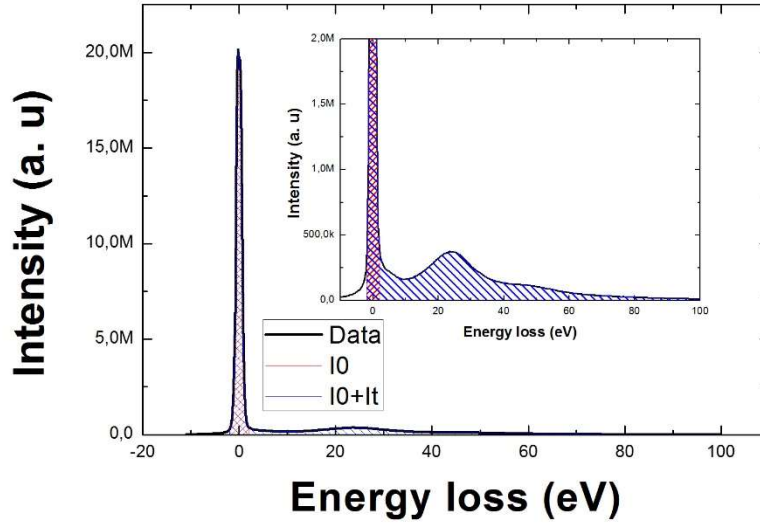


Figure 3: Low-loss EELS spectrum of a GO sample. Both the I_0 (red) and the I_t (blue) regions are shown.

Based on previous studies and experimental parameterisations on the matter^{1,7,8}, and taking into account that we are working at low acceleration voltages and low thicknesses ($t < 5\lambda$), the value of λ can be parameterised as

$$\lambda = \frac{106 \times F \times E_0}{E_m \times \ln\left(2\beta \times \frac{E_0}{E_m}\right)}$$

where F is a relativistic constant, E_0 is the incident energy, β is the microscope collection semi-angle, and E_m is an effective energy related to electron scattering that is defined as $E_m = 7.6 \times Z_{eff}^{0.36}$, where Z_{eff} is an effective atomic number that can be estimated from the composition analysis of the sample

$$Z_{eff} = \frac{\sum_i [i] \times Z_i^{1.3}}{\sum_i [i] \times Z_i^{0.3}}$$

where i represents each element present in the sample, $[i]$ its relative concentration and Z_i its atomic number.

Mass density estimation

The bibliography offers an expression for the mass density of the sample as a function that can be either measured directly or have been approximated in the literature^{9,10}, provided we only have trace amounts of elements other than nitrogen, and that even these are very small amounts (in other words, $X_C + X_O \approx 1$):

$$\rho = \frac{E_p^2 \times m^* \times \epsilon_0 \times \mu \times (12 + 4X_O)}{\hbar \times e^2 \times (4 + 2X_O)}$$

In this expression, m^* is the effective electron mass that has been approximated in the literature for this kind of materials as $m^* = 0.87 \times m_e$; μ is an atomic mass parameter defined as $\mu = \frac{M_C}{12 \cdot N_A}$, where M_C is the molecular weight of carbon and N_A is Avogadro's number.

As for E_p , this value refers to the plasmon energy of the material itself, which can be estimated by performing a Drude fit on the $\pi + \sigma$ plasmon spectral region in the low-loss spectrum (determined by the spectral window, where the intensity of the plasmon peak is over 70% of the maximum intensity of the feature):

$$I_{LLEELS} \propto \text{Im} \left(-\frac{1}{\epsilon(E)} \right) = \frac{E_p^2 \times E \times \Delta E_p}{(E^2 - E_p^2)^2 + (E \times \Delta E_p)^2}$$

In the case of thin ($t < 10$ nm) and reduced samples, a double fit has been performed to account for both features. An example for both fits can be seen in Figure 4.

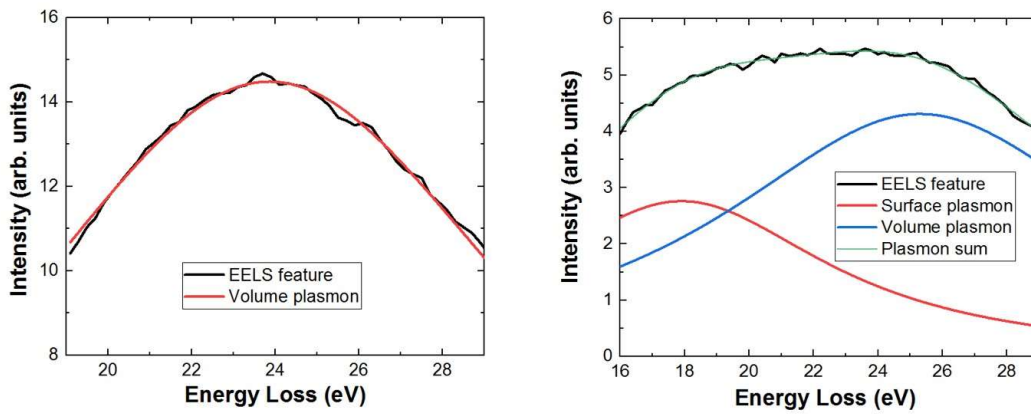


Figure 4: Drude model fitting of the low-loss EEL spectra. Left: single fit of a GO sample with no visible surface plasmonic feature. Right: double fit of a rGO sample with a visible surface plasmonic feature (red) as well as a volume plasmonic feature (blue).

sp² fraction estimation

The estimation of the fraction of the C atoms in the sample that present *sp*² hybridisation (that is, graphene-like carbon) is estimated using the C-K edge of the core-loss EEL spectra. For amorphous samples, the *sp*² fraction in the sample is proportional to the relative intensity of the π^* feature with respect to the sum of the π^* and σ^* features in said edge. This ratio is known as y' . It is known from the literature that, for the experimental conditions in the studies ($\alpha = 0.5, \beta = 19.7$), the value of y' for a 100% *sp*² sample is 0.2^{9,11}, so for any amorphous sample the *sp*² fraction is estimated as:

$$\%sp^2 = \frac{y'_s}{y'_{100}} \times 100 = \frac{y'_s}{0.2} \times 100$$

Where y'_s is the y' ratio estimated from the core-loss spectra of the sample.

For this estimation, a spectral region is selected from 280 eV to 3 eV over the local minimum between the π^* feature and the σ^* feature. The σ^* feature has been fitted by means of a Gaussian fit centered at 294 eV, while the π^* feature has been fitted with an exponentially decreasing series of 60 Gaussians to account for its spectral tail^{11,12}. The Gaussian sum used for this particular fit is as follows:

$$I = h \times \sum_{i=0}^{60} 0.7^i \times e^{-\frac{(x-x_0-0.5 \cdot i)^2}{\sigma^2}}$$

with h being proportional to the height of the initial Gaussian, x_0 being the position of the initial Gaussian and σ being proportional to the FWHM of the Gaussians employed. An example of a spectrum featuring the Gaussian sum fit for the π^* feature can be seen in Figure 5.

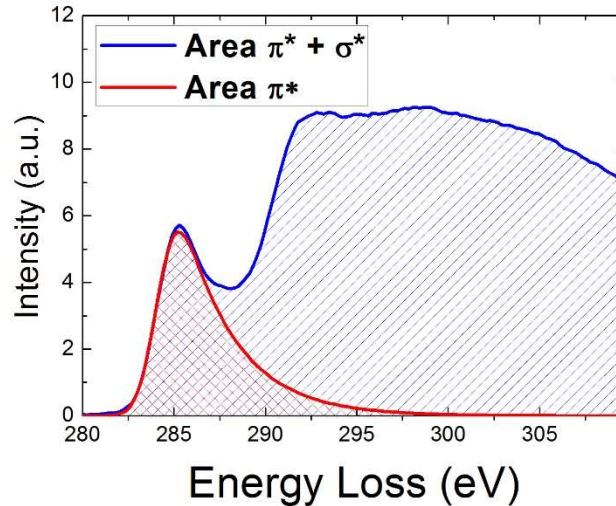


Figure 5: Gaussian sum fit of the π^ feature of the C-K edge in GO. The red striped area represents the integrated intensity of this feature in the energy window of interest, and the blue striped area the integrated intensity of the whole spectrum in this energy window.*

In the case of heavily oxidised samples, where the fine structure features associated with the OFGs present in the sample are intense enough to interfere with this analysis, additional

Gaussian fits have been put in place to account for these features. An example of this analysis can be seen in Figure 6.

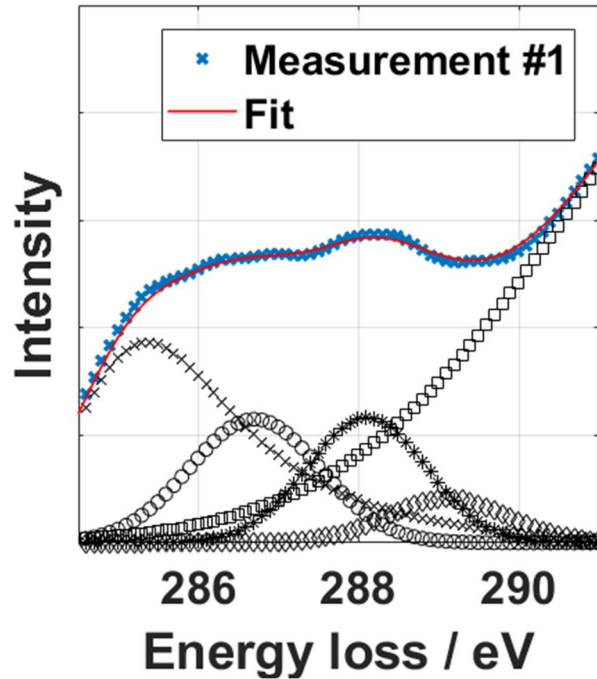


Figure 6: Gaussian sum fit of the π^* feature in the GO C-K edge (black crosses) as well as Gaussian fits related to OFG ELNES features (circles, asterisks and diamonds).

The value of γ' has been calculated as the ratio between the integrated intensity of this Gaussian sum in the spectral window of 280-310 eV and the integrated intensity of the whole C-K edge in this same spectral window.

As it has been mentioned, this method, under these experimental acquisition conditions, is only accurate for amorphous carbonaceous materials, that is, isotropic samples. In the case of graphene-like samples, the high anisotropy of the material leads to orientation effects that result in an important underestimation of the sp^2 fraction. For this reason, an MLLS approach has been used for these samples, fitting each spectrum with two spectra of which its sp^2 fraction value was known. These two references have been, respectively, a spectrum of GO at 70 °C and a reference spectrum of HOPG, of which we assumed a sp^2 fraction of 100%, both with similar thickness.

After normalisation, the spectra were cut to an energy window between 280 and 290 eV and fitted with the two known references, which were approximated with a multi-Gaussian fit to reduce noise. In this sense, each spectrum can be expressed as a linear combination of the two reference spectra or, in this case, a linear combination of their Gaussian decompositions:

$$S = a \times S_{GO} + b \times S_{HOPG} = a \times \sum_1^8 G_{GO} + b \times \sum_1^8 G_{HOPG}$$

Once the fit has provided the values for a and b, it is possible to calculate the value for the sp^2 fraction:

$$\%sp^2 = \frac{a \times \%sp^2_{GO} + b \times \%sp^2_{HOPG}}{a + b}$$

An example of this fit can be seen in Figure 7.

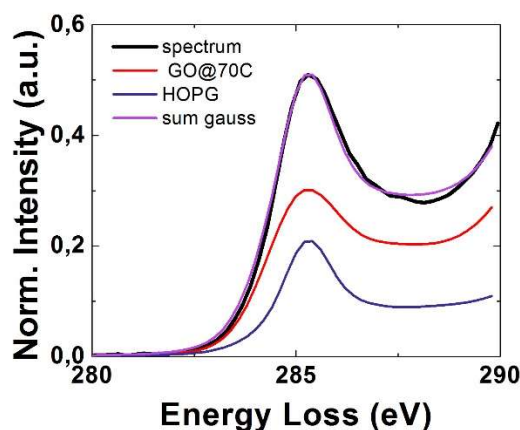


Figure 7: MLLS fit of a highly reduced GO sample using an amorphous GO spectrum and an HOPG spectrum.

REFERENCES

- (1) Egerton, R. F. *Electron Energy-Loss Spectroscopy in the Electron Microscope*, 3rd ed.; Springer US: Boston, MA, 2011. <https://doi.org/10.1007/978-1-4419-9583-4>.
- (2) D'Angelo, D.; Bongiorno, C.; Amato, M.; Deretzis, I.; la Magna, A.; Compagnini, G.; Spanò, S. F.; Scalese, S. Electron Energy-Loss Spectra of Graphene Oxide for the Determination of Oxygen Functionalities. *Carbon* **2015**, *93*, 1034–1041. <https://doi.org/10.1016/J.CARBON.2015.06.025>.
- (3) D'Angelo, D.; Bongiorno, C.; Amato, M.; Deretzis, I.; la Magna, A.; Fazio, E.; Scalese, S. Oxygen Functionalities Evolution in Thermally Treated Graphene Oxide Featured by EELS and DFT Calculations. *The Journal of Physical Chemistry C* **2017**, *121* (9), 5408–5414. <https://doi.org/10.1021/acs.jpcc.7b00239>.
- (4) Tararan, A.; Zobelli, A.; Benito, A. M.; Maser, W. K.; Stéphan, O. Revisiting Graphene Oxide Chemistry via Spatially-Resolved Electron Energy Loss Spectroscopy. *Chemistry of Materials* **2016**, *28* (11), 3741–3748. <https://doi.org/10.1021/acs.chemmater.6b00590>.
- (5) Pelaez-Fernandez, M.; Bermejo, A.; Benito, A. M.; Maser, W. K.; Arenal, R. Detailed Thermal Reduction Analyses of Graphene Oxide via In-Situ TEM/EELS Studies. *Carbon* **2021**, *178*, 477–487. <https://doi.org/10.1016/j.carbon.2021.03.018>.
- (6) Hettler, S.; Sebastian, D.; Pelaez-Fernandez, M.; Benito, A. M.; Maser, W. K.; Arenal, R. In-Situ Reduction by Joule Heating and Measurement of Electrical Conductivity of Graphene Oxide in a Transmission Electron Microscope. *2D Materials* **2021**, *8* (3). <https://doi.org/10.1088/2053-1583/abcdc9>.

- (7) Wang, F.; Egerton, R.; Malac, M. Fourier-Ratio Deconvolution Techniques for Electron Energy-Loss Spectroscopy (EELS). *Ultramicroscopy* **2009**, *109* (10), 1245–1249. <https://doi.org/10.1016/j.ultramic.2009.05.011>.
- (8) Malis, T.; Cheng, S.; Egerton, R. F. EELS Log-Ratio Technique for Specimen-Thickness Measurement in the TEM. *Journal of Electron Microscopy Technique* **1988**, *8* (May 2016), 193–200. <https://doi.org/10.1002/jemt.1060080206>.
- (9) Ferrari, A. C.; Libassi, A.; Tanner, B. K.; Stolojan, V.; Yuan, J.; Yuan, J.; Brown, L. M.; Rodil, S. E.; Kleinsorge, B.; Robertson, J. Density, Sp³ Fraction, and Cross-Sectional Structure of Amorphous Carbon Films Determined by x-Ray Reflectivity and Electron Energy-Loss Spectroscopy. *Physical Review B - Condensed Matter and Materials Physics* **2000**, *62* (16), 11089–11103. <https://doi.org/10.1103/PhysRevB.62.11089>.
- (10) Liu, A. C. Y.; Arenal, R.; Chen, X. Clustering in a Highly Hydrogenated Diamondlike Carbon Determined Using Fluctuation Electron Microscopy and Phenomenological Atomistic Simulations. *Physical Review B - Condensed Matter and Materials Physics* **2007**, *76* (12), 1–4. <https://doi.org/10.1103/PhysRevB.76.121401>.
- (11) Lajaunie, L.; Pardanaud, C.; Martin, C.; Puech, P.; Hu, C.; Biggs, M. J.; Arenal, R. Advanced Spectroscopic Analyses on a:C-H Materials: Revisiting the EELS Characterization and Its Coupling with Multi-Wavelength Raman Spectroscopy. *Carbon* **2017**, *112*, 149–161. <https://doi.org/10.1016/j.carbon.2016.10.092>.
- (12) Bernier, N.; Bocquet, F.; Allouche, A.; Saikaly, W.; Brosset, C.; Thibault, J.; Charai, A. A Methodology to Optimize the Quantification of Sp²carbon Fraction from K Edge EELS Spectra. *Journal of Electron Spectroscopy and Related Phenomena* **2008**, *164* (1–3), 34–43. <https://doi.org/10.1016/j.elspec.2008.04.006>.

D6.2.2 In-situ EELS investigations of metal/insulating transitions - Orsay:

ORS studied the temperature-activated metal (PM) to insulating (AFI) transition (MIT) in V_2O_3 nanostructures. Low-T thermal cycles across the electronic transition, i.e. 135 - 165 K, were monitored for probing and mapping the PM and AFI spectroscopic signatures using UHR (ultra high-resolution) STEM-EELS. Initially, Abe *et al.* performed low-loss and core-loss EELS at specific temperatures evidencing (i) a sharp spectral feature at ca. 1 eV in the PM state attributed to an interband plasmon that vanishes in the AFI phase and (ii) an energy shift of ca. 500meV on the O-K edge between PM and AFI states associated with a decrease in intensity in AFI related to the lower $V3d - O2p$ hybridization [1]. The experiments were performed on the CHROMATEM microscope equipped with a double-tilt HennyZ stage cryo-holder providing variable temperature (from 110K).

First, the EELS low-loss signatures upon cooling and warming enabled us to highlight the temperature range of both electronic phases (Fig. 2.a) and a 15K hysteresis between the MIT and IMT. Furthermore, the low-loss PM and AFI signatures were mapped at the sub-nm scale upon thermal cycling confirming the coexistence of I/M nanodomains limited here by an electronic domain wall (Fig. 2.b). K-means clustering analyses [10,11] were applied on the low-loss hyperspectral data confirming an electronic homogeneity of each PM/AFI domains (Fig 2.c and 2.d). Upon heating, the electronic nanodomains switching can be observed dynamically over few degrees by following the propagation of the electronic domain wall, which tends from insulating to metallic. In addition, *in-situ* 4DSTEM experiments also performed during the thermal cycles revealed the structural evolution of these I/M domains across the phase transition.

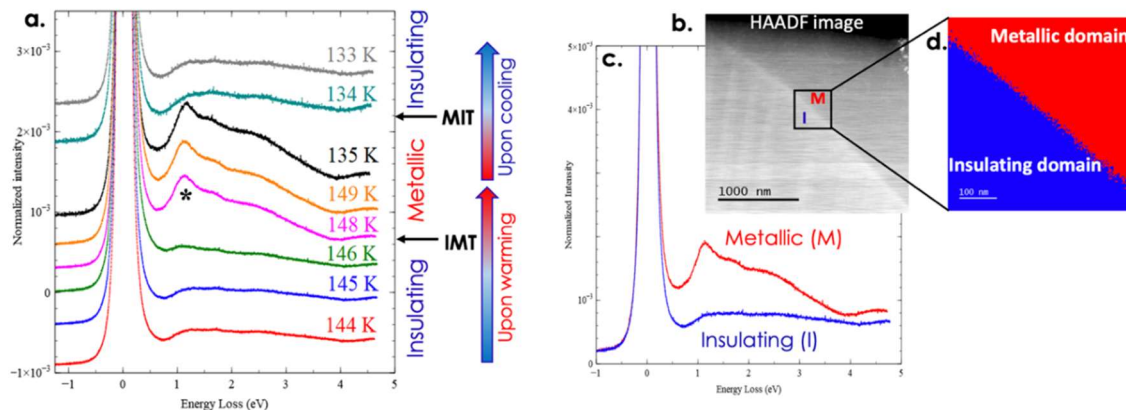


Fig. a. EELS spectra acquired in the low-loss domain (sum of 2000 spectra of 100ms) probed every 1K across the resistive transition while cooling and heating. * indicated the characteristic peak at ca. 1.eV solely present in the metallic phase. **b.** STEM-HAADF image acquired at 147 K, the associated hyperspectral data were acquired in the region of interest (black square). **c.** EELS spectra extracted in the I/M domains among the region of interest, **d.** map of the electronic coexistence at the I/M domain wall at 147 K et obtained par the K-means clustering method.

[1] Hiroyuki Abe, et al. Electron Energy-Loss Spectroscopy Study of the Metal-Insulator Transition in V_2O_3 . *Jpn. J. Appl. Phys.* **37**, 584 (1998).